

Illumination Correction in Dermatological Photographs using Multi-stage Illumination Modeling for Skin Lesion Analysis

Jeffrey Glaister, Alexander Wong, David A. Clausi

Abstract—A novel algorithm for correcting illumination variation in dermatological photographs via a multi-stage modeling of the underlying illumination is proposed for the purpose of skin lesion analysis. First, an initial illumination estimate is obtained via a non-parametric modeling strategy based on Monte Carlo sampling. Next, a subset of pixels from the non-parametric estimate is used to determine a parametric estimate of the illumination based on a quadratic surface model. Using the parametric illumination estimate, the reflectance map is obtained and used to correct the photograph. The photographs corrected using the proposed algorithm are compared to uncorrected photographs and to a state-of-the-art correction algorithm. Qualitatively, a visual comparison is performed, while quantitatively, the coefficient of variation of skin pixel intensities is calculated and the precision-recall curve for segmentation of skin lesions is graphed. Results show that the proposed algorithm has a lower coefficient of variation and an improved precision-recall curve.

I. INTRODUCTION

Melanoma is a form of skin cancer frequently found on the back or legs [1]. One in 74 men and one in 90 women are expected to develop it during their lifetime, and it is the most serious type of skin cancer. Melanoma causes the majority of deaths from skin cancer, but can be treated if detected early [2]. Unfortunately, the incidence of melanoma, especially among young men, is increasing, and the costs and time required for dermatologists to check all patients for melanoma is prohibitively expensive. There is a need for an automated system to assess a patient's risk of melanoma, using the patient's background and photographs of skin lesion.

To automatically analyze photographs of skin lesions to screen for melanoma, the photographs must be preprocessed to correct for illumination variation which causes areas of the skin to appear with greatly differing pixel intensities. Fig. 1a shows an example of a photograph of skin lesion with large illumination variation. This becomes problematic when trying to perform segmentation and feature extraction on the photograph, as dark areas of skin can be misclassified as skin lesion.

While several algorithms to correct for illumination variation have been proposed, few have been applied to correcting skin lesion photographs. General illumination correction algorithms are based on the illumination-reflectance

model, histogram equalization, or morphological operators. The illumination-reflectance model assumes that there is a multiplicative relationship between illumination and reflectance [3] and uses Gaussian filtering of differing sizes in the logarithmic space to estimate the illumination model component [4]. An adaptive Monte Carlo sampling approach to finding the illumination map has been proposed [5]. Histogram equalization adjusts pixel intensities based on the global distribution to reduce illumination variation [6]. Finally, morphological operators estimate local illumination and assume a similar illumination-reflectance model [7]. Morphological operators have been applied to correct photographs of skin lesions, where a state-of-the-art algorithm also fit the illumination map to a parabolic surface as a parametric model [8] [9]. However, the state-of-the-art algorithm proposed by Cavalcanti et al. only uses a small subset of the illumination map when fitting the surface [9].

In this paper, a novel algorithm to correct for illumination variation in photographs of skin lesions by estimating the underlying illumination via multi-stage modeling is proposed for the purpose of skin lesion analysis. The proposed algorithm follows three stages. First, an initial estimate of the illumination map is found using non-parametric modeling based on a Monte Carlo sampling approach. Second, a final estimate of the illumination map is determined via parametric modeling based on a quadratic surface model, using the non-parametric map as a prior. Finally, the reflectance is estimated based on the final illumination estimate and used to remove illumination variation.

II. METHODOLOGY

In this section, the three stages of the algorithm are explained. First, the problem formulation is derived and Monte Carlo sampling is applied to find the initial non-parametric illumination estimate. Second, a final parametric illumination estimate is determined based on a quadratic surface model using the initial estimate as a prior. Finally, the reflectance map is estimated and the corrected photograph is constructed.

A. Initial Non-parametric Modeling of Illumination

To perform illumination correction on the skin lesion photographs, it is first necessary to estimate the underlying illumination model from the skin lesion images. Let the V (value) channel from the skin lesion photographs in the HSV (hue-saturation-value) colour space be modeled as the entrywise product of illumination i and reflectance r . This relationship can be expressed in an additive form in the

This work was supported by the Natural Sciences and Engineering Research Council of Canada and the Ontario Ministry of Economic Development and Innovation.

Jeffrey Glaister, Alexander Wong and David A. Clausi are part of the Vision and Image Processing Lab with the Department of Systems Design Engineering, University of Waterloo, Ontario, Canada, N2L 3G1. {jlglaist, a28wong, dclausi}@uwaterloo.ca

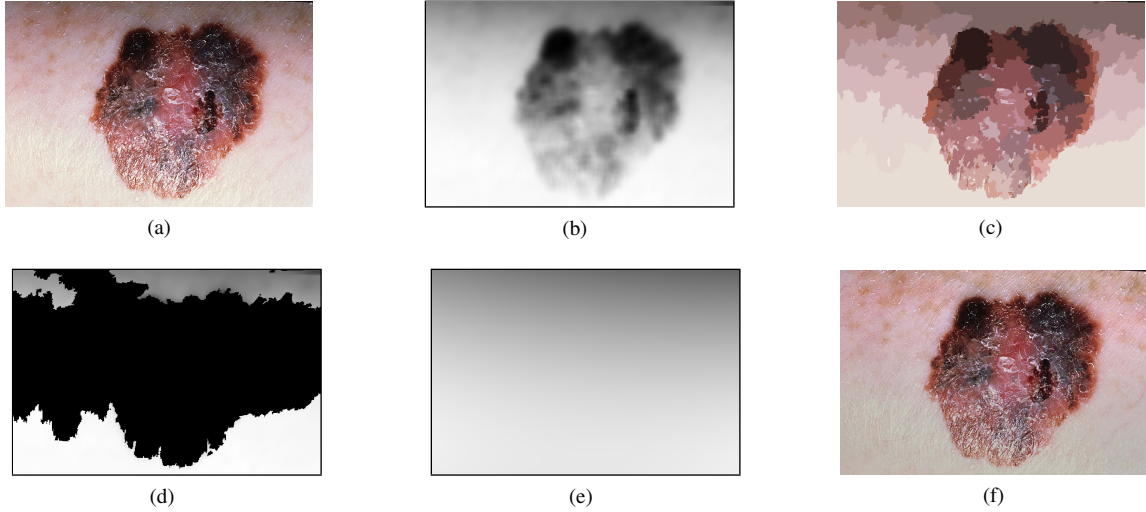


Fig. 1: Methodology to estimate illumination map: (a) original photograph of a skin lesion, where the top edge is noticeably darker than the bottom edge; (b) illumination map determined via non-parametric modeling using Monte Carlo sampling; (c) segmentation map found using statistical region merging; (d) regions included in the subset of skin pixels, where pixels black in colour are not classified as normal skin; (e) new illumination map determined by using (d) as a prior to the quadratic surface model; (f) resulting corrected photograph using the proposed illumination correction algorithm.

logarithmic space (1). Only the V channel is corrected because it is assumed that the photograph is taken indoors in an office, in a controlled environment, during a dermatology exam, and underneath white light.

$$\begin{aligned} v(x, y) &= i(x, y) \cdot r(x, y) \\ v_{log}(x, y) &= i_{log}(x, y) + r_{log}(x, y) \end{aligned} \quad (1)$$

The estimation of i can be seen as the inverse problem and formulated as Bayesian least squares, where $p(i_{log}|v_{log})$ is the posterior distribution (2).

$$\begin{aligned} \hat{i}_{log} &= \arg \min_{i_{log}} \{E(i_{log} - \hat{i}_{log})^2 | v_{log}\} \\ &= \arg \min_{i_{log}} \left(\int (i_{log} - \hat{i}_{log})^2 p(i_{log}|v_{log}) di_{log} \right) \end{aligned} \quad (2)$$

Due to the complexity of estimating a posterior distribution $p(i_{log}|v_{log})$, a Monte Carlo posterior estimation algorithm is used instead [10]. Furthermore, using Monte Carlo estimation avoids assuming a parametric model for the posterior distribution $p(i_{log}|v_{log})$ as it is a non-parametric approach. In the Monte Carlo estimation strategy used, candidate samples are drawn from a uniform instrumental distribution. An acceptance probability α is computed based on the candidate sample, and the candidate sample is accepted with a probability of α for estimating $p(i_{log}|v_{log})$. Then, an estimate of the log-transformed illumination map \hat{i}_{log} is calculated, as outlined in [11]. Taking the exponential of \hat{i}_{log} gives the initial illumination estimate \hat{i} (Fig. 1b).

B. Final Parametric Modeling of Illumination

The next stage is to find the final parametric illumination estimate via a parametric modeling process using a quadratic

surface model, with a subset of pixels from the initial non-parametric estimate as prior information. There are two reasons for doing this parametric modeling stage. First, a quadratic surface is assumed to adequately model illumination because the photographs are taken in controlled indoor environments with a single source of light. Second, the non-parametric illumination estimation approach is sensitive to outliers, particularly in the lesion area. Therefore, the quadratic surface is fit using only pixels belonging to the skin class.

The algorithm proposed by Cavalcanti et al. used 20×20 regions in the four corners of the illumination map as the set of skin pixels to use to estimate the surface [9]. Due to the small size of the regions, especially in high resolution photographs, this does not always result in a large enough set of pixels to accurately estimate the surface. Instead, the proposed algorithm segments the photograph using a Statistical Region Merging approach [12] and uses those segments to compute the surface model. These two steps are described in detail in the following sections.

1) *Statistical Region Merging*: To estimate pixels that belong to the skin or lesion class, the original colour photograph of the skin lesion is segmented. The segmentation algorithm used is the Statistic Region Merging (SRM) algorithm, as it was shown to perform well on colour images [12]. SRM tends to over-segment the image, but it still serves as a good estimate of segments which correspond to the skin class. After the image is segmented, any segment that touches the corners of the image is classified as normal skin and is added to the set S . This allows a larger set of skin pixels to be used to fit the quadratic surface.

2) *Quadratic Surface Modeling*: A quadratic surface model (3) is used, as proposed in [9].

$$i'(x, y) = P_1x^2 + P_2xy + P_3y^2 + P_4x + P_5y + P_6 \quad (3)$$

Based on this model, the final illumination map i' is then estimated by computing the parameters of the surface model using maximum likelihood estimation based on the initial estimate \hat{i} and the set of skin pixels S (4).

$$\hat{i}' = \arg \max_{\hat{i}'} \prod_{(x,y) \in S} P(\hat{i}(x, y) | \hat{i}'(x, y)) \quad (4)$$

$$\text{where } P(\hat{i}(x, y) | \hat{i}'(x, y)) \stackrel{\text{iid}}{\sim} \mathcal{N}(\hat{i}'(x, y), \sigma^2)$$

Fig. 1d-f show the segmentation map, subset of skin pixels, and the new illumination map based on the quadratic surface model.

C. Reflectance Map Estimation

Based on an HSV color space, the reflectance component is calculated by dividing the illumination (V) channel from the original colour photograph v by \hat{i}' . The resulting reflectance channel \hat{r} is substituted as the new V channel. The new channel is combined with the original hue (H) and saturation (S) channels to construct the new photograph, corrected for illumination variation. Fig. 1f shows a corrected photograph, following the steps defined in the Methodology section.

III. EXPERIMENTAL RESULTS

This section outlines the experimental results demonstrating the improved performance attained by correcting for illumination variation using the proposed algorithm. Furthermore, comparisons with the algorithm in [9] are shown. To compare the two algorithms, efforts were made of normalize the illumination corrected photographs. The average V channel values of skin class pixels in photographs corresponding to the two algorithms were adjusted to be the same. The ground truth segmentation, found manually, was used to classify the skin pixels. This allows a fair comparison as the images are adjusted to have a similar range of skin pixel intensities.

The photographs were first compared visually. To quantitatively measure the effect of illumination correction, the coefficient of variation is computed based on the skin pixels, which shows that illumination variation has decreased. Eight photographs tested were from the DermNet database [13] and two were from the DermQuest database [14]. Five examples of results comparing the illumination correction algorithms are shown in Fig. 2.

A. Segmentation Results

To compare the effect of illumination correction on processing of the photographs, the photographs were segmented using a pixel intensity threshold. The segmentation algorithm outlined in [9] was used, which has separate thresholds for the R, G, and B colour channels.

Because image statistics greatly impact the optimal threshold values selected, a subset of all possible threshold values

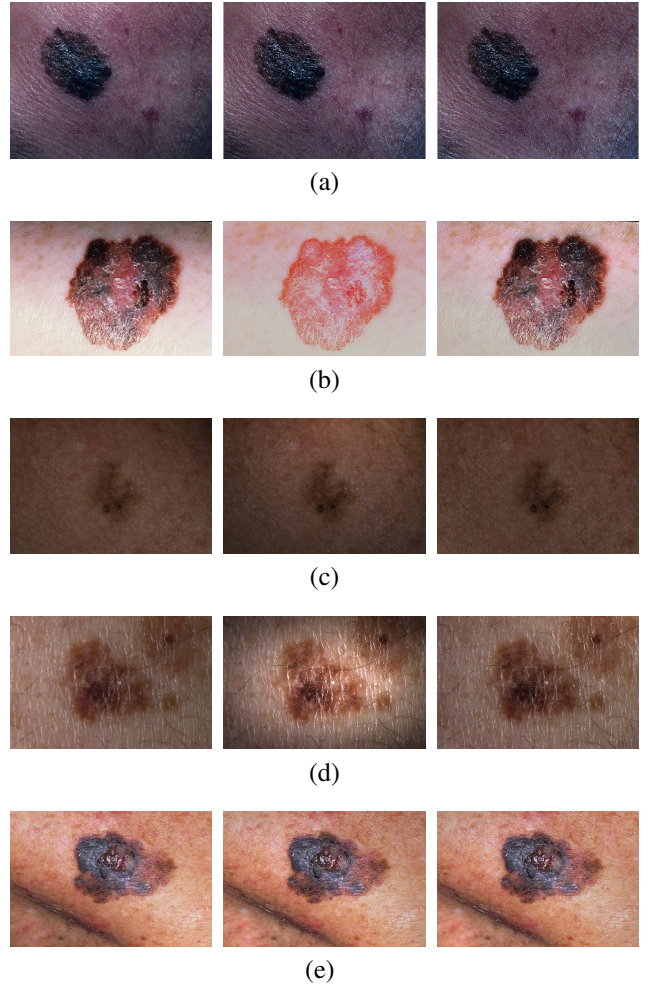


Fig. 2: Examples of illumination correction in dermatological photographs from the DermNet database [13]. First column is the original photograph. Second column is the illumination correction results using the algorithm outlined in [9]. Third column is the illumination correction result using the proposed MCMC algorithm.

for each channel is used as a more comprehensive analysis of the effect of the illumination correction algorithm on segmentation that is independent from selecting of a single threshold. Classification based on those thresholds is performed, the precision and recall values are calculated and the recall-precision curve is fit. The recall-precision curves for example photographs (Fig. 2a and b) are graphed in Fig. 3.

Similar curves were found for most photographs tested. The recall-precision curves for the proposed algorithm are higher than those of the algorithm in [9] and the uncorrected photograph. This means that for a given recall value, the corresponding precision value for the proposed algorithm is higher.

B. Visual Comparison Results

Fig. 2 show examples comparing the uncorrected and corrected photographs. Fig. 2a-d are cases where the proposed algorithm looks visually better, compared to the original

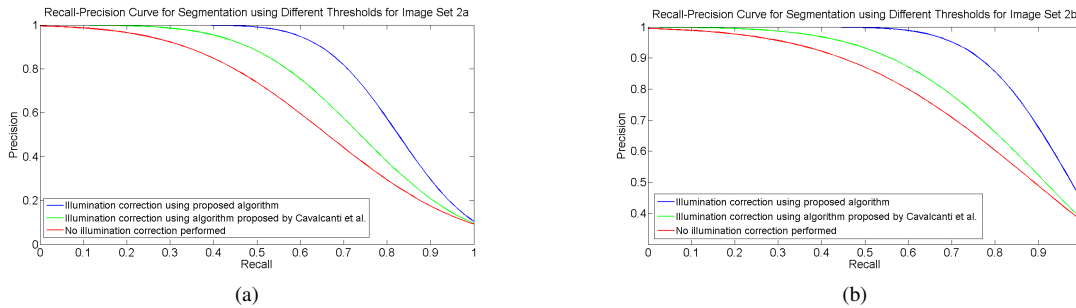


Fig. 3: Precision-recall curves corresponding to segmentation results using different thresholds for Fig. 2a and b.

TABLE I: Coefficient of variation of normal skin pixels.

Photograph	Original Photograph	Corrected Photograph	
		Cavalcanti et al. Approach	Proposed Approach
a	0.300	0.242	0.197
b [†]	0.206	0.001	0.064
c	0.143	0.217	0.105
d	0.211	0.312	0.130
e	0.152	0.153	0.193
f	0.185	0.164	0.165
g	0.240	0.211	0.076
h	0.309	0.260	0.1702
i	0.316	0.363	0.320
j	0.274	0.290	0.430

[†]For photograph b, the Cavalcanti et al. approach produces a very low C value, but the skin lesion and normal skin are less separable, as seen in Fig. 2b and 3b.

photograph and the corrected photograph using the algorithm from [9]. Fig. 2e is an example where the proposed algorithm fails to adequately correct the photograph. The illumination variation is difficult to correct as the parametric model of the illumination is assumed to be a smooth quadratic surface. In reality, it is not because the illumination sharply decreases due to the shadow of one limb on top of another limb.

C. Coefficient of Variation Results

The coefficient of variation is a metric that compares the ratio of standard deviation and the mean of a set of values, and has been used to quantify illumination correction [15]:

$$C = \frac{\sigma}{\mu} \quad (5)$$

To calculate the coefficient of variation (C), the standard deviation σ and mean μ of the V channel intensities of pixels classified as normal skin were used. To determine classification, the photographs were manually segmented. A lower C is more ideal, as illumination correction attempts to remove variations in the V channel intensities, leaving only variations due to skin texture.

The C values for the tested photographs are listed in Table I. For most photographs, using the proposed algorithm decreases the variance of skin pixel intensities compared to the uncorrected photograph and the algorithm from [9]. Images a-e correspond to the images shown in Fig. 2. Boldface indicates which method produced the photograph with the lowest C .

IV. CONCLUSION

This paper presented an algorithm to correct for illumination variance in dermatological photographs for the purpose of skin lesion analysis. Preliminary results found that in most cases the proposed algorithm had lower coefficient of variation and better precision-recall curves, which show potential for improved skin lesion analysis. Further work is to be done to test the algorithm on a larger set of photographs, as well as determine alternative models for improving illumination modeling.

REFERENCES

- [1] Public Health Agency of Canada, *Melanoma Skin Cancer*, http://www.phac-aspc.gc.ca/cd-mc/cancer/melanoma_skin_cancer-cancer_peau_melanome-eng.php, accessed Dec 7, 2011.
- [2] A. R. Rhodes, *Public Education and Cancer of the Skin: What Do People Need to Know about Melanoma and Nonmelanoma Skin Cancer?*, *Cancer*, vol. 75, no. 2, pp. 613-636, October 1994.
- [3] E. Land and J. McCann, *Lightness and Retinex Theory*, *J. Optical Soc. of America*, vol. 61, pp. 1-11, 1971.
- [4] D. J. Jobson, Z. Rahman, and G. A. Woodell, *A Multi-Scale Retinex For Bridging the Gap Between Color Images and the Human Observation of Scenes*, *IEEE Transactions on Image Processing: Special Issue on Color Processing*, vol. 6, issue 7, pp. 965-976, July 1997.
- [5] A. Wong, D. A. Clausi, and P. Fieguth, *Adaptive Monte Carlo Retinex Method for Illumination and Reflectance Separation and Color Image Enhancement*, *Canadian Conference on Computer and Robot Vision*, pp. 108-115, May 2009.
- [6] S. Shan, W. Gao, B. Cao and D. Zhao, *Illumination normalization for robust face recognition against varying lighting conditions*, *IEEE International Workshop on Analysis and Modeling of Faces and Gestures*, pp. 157-164, October 2003.
- [7] P. Soille. "Morphological operators" in *Handbook of Computer Vision and Applications* vol. 2. B. Jahne, H. Hauecker, and P. Geiler, Ed., San Diego: Academic Press, 1999, pp. 627-682.
- [8] P. G. Cavalcanti and J. Scharcanski, *Automated prescreening of pigmented skin lesions using standard cameras*, *Computerized Medical Imaging and Graphics*, vol. 35, issue 6, pp. 481-491, September 2011.
- [9] P. G. Cavalcanti, J. Scharcanski, and C. Lopes, *Shading Attenuation in Human Skin Color Images*, *Lecture Notes in Computer Science: Advances in Visual Computing*, pp. 190-198.
- [10] M. Chen, *Importance-Weighted Marginal Bayesian Posterior Density Estimation*, *Journal of the American Statistical Association*, vol. 89, no. 427, pp. 818- 824, September 1994.
- [11] P. Fieguth, *Statistical Image Processing and Multidimensional Modeling*, New York, NY: Springer, 2011, pp 65.
- [12] R. Nock and F. Nielsen, *Statistical region merging*, *IEEE Transactions on Pattern Analysis and Machine Intelligence*, vol. 26, issue 11, pp. 1452-1458, November 2004.
- [13] DermNet Skin Disease Image Atlas, <http://www.dermnet.com>.
- [14] DermQuest Database, <http://www.dermquest.com>.
- [15] E. Ardicione, R. Pirrone and O. Gambino, *Illumination Correction on MR Images*, *Journal of Clinical Monitoring and Computing*, vol. 20, issue 6, pp. 391-398, July 2006.